

123. Synthesis of 2'-Deoxy-5-(isothiazol-5-yl)uridine and Its Interaction with the HSV-1 Thymidine Kinase

by Ingrid Luyten^{a)}, Hans De Winter^{a)}, Roger Busson^{a)}, Theo Lescrier^{a)}, Isabelle Creuven^{c)}, François Durant^{c)}, Jan Balzarini^{b)}, Erik De Clercq^{b)}, and Piet Herdewijn^{a)*}

^{a)} Laboratory for Medicinal Chemistry and ^{b)} Laboratory of Virology and Chemotherapy,

Rega Institute for Medical Research, Katholieke Universiteit Leuven, Minderbroederstraat 10, B-3000 Leuven

^{c)} Laboratoire de Chimie Moléculaire Structurale, Facultés Universitaires N.-D. de la Paix, rue de Bruxelles 61, B-5000 Namur

(13. II. 96)

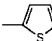
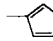
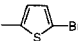
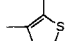
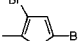
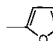
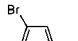
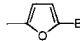
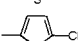
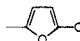
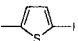
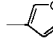
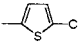
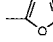
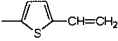
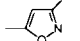
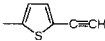
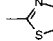
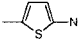
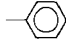
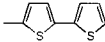
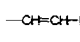
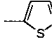
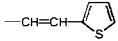
2'-Deoxy-5-(isothiazol-5-yl)uridine (**12**) was synthesized starting from 2'-deoxy-5-iodouridine using a Pd-catalysed cross-coupling reaction with propionaldehyde diethyl acetal followed by deprotection and ring closure using thiosulfate. 2'-Deoxyuridine **12** has a particular place among the 5-heteroaryl-substituted 2'-deoxyuridines in that it has a high affinity for herpes simplex virus type 1 (HSV-1)-encoded thymidine kinase (TK) without antiviral activity. Biochemical studies revealed that **12** is a substrate for viral TK. We further investigated the interaction of **12** with the HSV-1 thymidine kinase. The conformation of **12** in solution was established by NMR spectroscopy. The most stable conformer **12A** has the S-atom of the isothiazole ring placed in the neighbourhood of the C(4)=O group of the pyrimidine moiety. The compound was docked in its most stable conformation in the active site of HSV-1 TK and subjected to energy minimization. This demonstrated that the isothiazole moiety binds in a cavity lined by the side chains of Tyr-132, Arg-163, Ala-167, and Ala-168 and that the C(3) atom of the isothiazole moiety is located in close proximity of the phenolic O-atom of Tyr-132 and the aliphatic part of the Arg-163 side chain.

Introduction. – The structure-activity-relationship study of 5-substituted 2'-deoxyuridines started with the historical discovery of 2'-deoxy-5-iodouridine as an anti-herpes agent [1]. The mode of action of 5-substituted 2'-deoxyuridines has since long been studied, and it is well documented that these compounds have to be phosphorylated to their mono-, di-, and triphosphate and that these metabolites are responsible for the biological activity. In their monophosphate form, some 5-substituted 2'-deoxyuridines are efficient inhibitors of thymidylate synthase [2]. In their triphosphate form, these nucleosides interfere with DNA synthesis by inhibiting DNA polymerases and/or by functioning as alternative substrates thus being incorporated into DNA. Whatever the mechanism, the first step in the anabolism to the active metabolite is the phosphorylation by nucleoside kinases. With respect to the 5-substituted 2'-deoxyuridines that are active against HSV-1, this phosphorylation is carried out by the viral thymidine kinase. The thymidine kinase (TK) encoded by herpes simplex virus type 1 (HSV-1) has a broader substrate specificity than the human enzymes so that modified nucleosides can be selectively activated in the HSV-1-infected cells.

Recently, a study was undertaken to analyse the affinity of several 5-substituted 2'-deoxyuridines for the HSV-1-encoded TK and to relate this affinity with structural data [3–8]. In *Table 1*, an overview is given of the compounds synthesized (see *Scheme* for general *Formula*), together with their TK affinity. Compounds with a low affinity for the

HSV-1 TK may demonstrate either high anti-HSV-1 activity (**3**, **4**, **6**, **16**, **17**, and **24**) or low anti-HSV-1 activity (**11**, **14**, **19**, **20**, and **22**). Compounds with a high affinity for the HSV-1 TK (**1**, **2**, **5**, **7**, **13**, **15**, **18**, and **23**) generally demonstrate high anti-HSV-1 activity with one exception: 2'-deoxy-5-(isothiazol-5-yl)uridine (**12**). In an effort to better understand the interaction of these 5-substituted 2'-deoxyuridines with the viral TK, some compounds were subjected to physicochemical studies. The products that were most intensively studied could be divided in a group of compounds with high affinity for the HSV-1 TK (*i.e.*, 2'-deoxy-5-(thien-2-yl)uridine (**1**), 5-(5-bromothien-2-yl)-2'-deoxyuridine (**2**), 5-(5-chlorothien-2-yl)-2'-deoxyuridine (**5**), and 2'-deoxy-5-(furan-2-yl)uridine (**15**)) and a group of compounds with low affinity for the enzyme (*i.e.*, 5-(3-bromothien-2-yl)-2'-deoxyuridine (**4**), 5-(5-bromofuran-2-yl)-2'-deoxyuridine (**16**), 2'-deoxy-5-(isoxazol-5-yl)uridine (**19**), and 5-(3-bromoisoxazol-5-yl)-2'-deoxyuridine (**20**)). This study led to the conclusion that the conformation of the molecules is highly influenced by possible S/C=O interactions [6] (*Fig. 1*), and that a substitution zone exists for unfavourable interactions

Table 1. Anti-HSV-1 Activity and Affinity for HSV-1 Thymidine Kinase of Different 2'-Deoxyuridines with a Heteroaryl Substituent in the 5-Position [3–5] [7]

5-Substituent	HSV-1 (Kos) replication EC_{50}^a [μ M]	HSV-1 Thymidine kinase IC_{50}^b [μ M]	5-Substituent	HSV-1 (Kos) replication EC_{50}^a [μ M]	HSV-1 Thymidine kinase IC_{50}^b [μ M]
1 	0.6	2.4	13 	1.0	4
2 	0.08	3.5	14 	2	143
3 	0.7	62.5	15 	1.5	2.9
4 	0.04	61.4	16 	0.4	51
5 	0.06	2.3	17 	0.6	28
6 	0.09	16	18 	1.7	1.5
7 	0.6	2.3	19 	68	36
8 	3.0	n.d. ^{c)}	20 	19	34
9 	1.2	n.d. ^{c)}	21 	64	n.d. ^{c)}
10 	5.6	n.d. ^{c)}	22 	–	102
11 	2	71	23 	0.02	0.3
12 	> 10	3.1	24 	0.07	50

^{a)} 50% effective concentration, or compound concentration required to inhibit HSV-1-induced cytopathicity in E₆SM cell cultures by 50%. ^{b)} 50% inhibitory concentration, or compound concentration required to inhibit HSV-1-TK activity by 50%. ^{c)} n.d. = not determined.

with the enzyme [8] (Fig. 2). Indeed, the solid-state conformation of the 5-substituted 2'-deoxyuridines (Fig. 1) is stabilized by either H-bonding (Figs. 1, a, c, e, and f) or S/C=O interaction (Fig. 1, b and d), leading to pseudo six-membered and pseudo five-membered rings, respectively. These stabilization effects are responsible for the orientation of the substituents on the heterocyclic five-membered ring, placing them either in the upper part of the molecule (Fig. 2: favourable interactions) or in the lower part of the

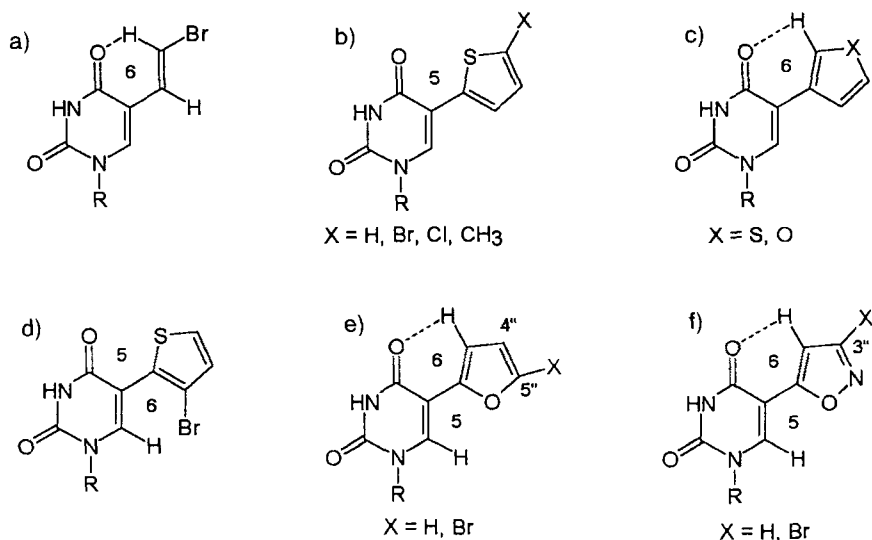


Fig. 1. Solid-state conformation of some 5-substituted 2'-deoxyuridines

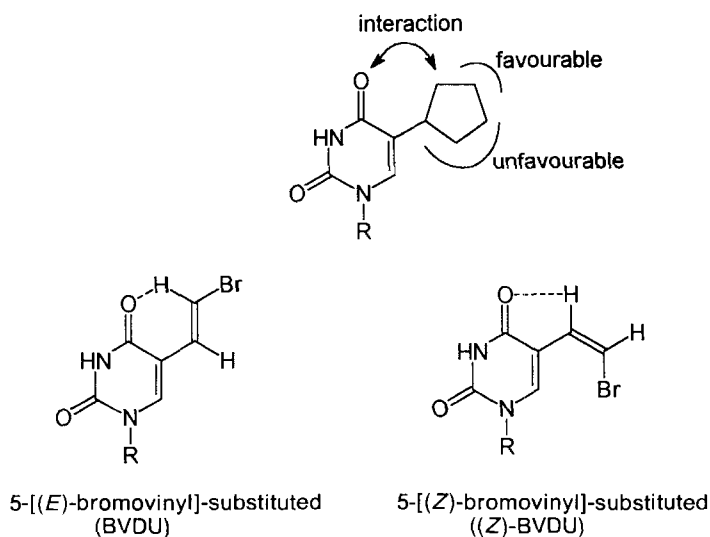


Fig. 2. Influence of the substitution sites for high affinity for viral TK

molecule (*Fig. 2*: unfavourable interactions). This theory agrees with previous observations that the (*E*)-configured BVDU is a highly active antiviral, whereas (*Z*)-BVDU is not [9] (BVDU = (*E*)-5-(bromovinyl)-2'-deoxyuridine (**23**)).

The X-ray analysis of the above mentioned compounds (**1**, **2**, **4**, **5**, **15**, **16**, **19**, **20**) has been confirmed by minimum-energy calculations (data not shown). Moreover, a correlation could be found between the electrostatic potential energy map, 1.75 Å above the plane of the bisheterocyclic system, of the compounds and their affinity for the enzyme [6]. This is illustrated in *Fig. 3* with two examples. In compounds with high affinity for the enzyme, an attractive region is observed above the C(4)=O function and the heteroaromatic five-membered ring and a repulsive zone above the pyrimidine ring (*Fig. 3, a*). The repulsive zone is extended over the whole bisheterocyclic system in compounds with low affinity for the HSV-1 TK (*Fig. 3, b*). In the plane of the compounds with high affinity, two attractive zones are present, induced by the C=O groups of the uracil ring [6]. The active compounds possess a dipole moment in the order of $\mu = 4.0$ D and an orientation comparable with that of the (*E*)-configured BVDU.

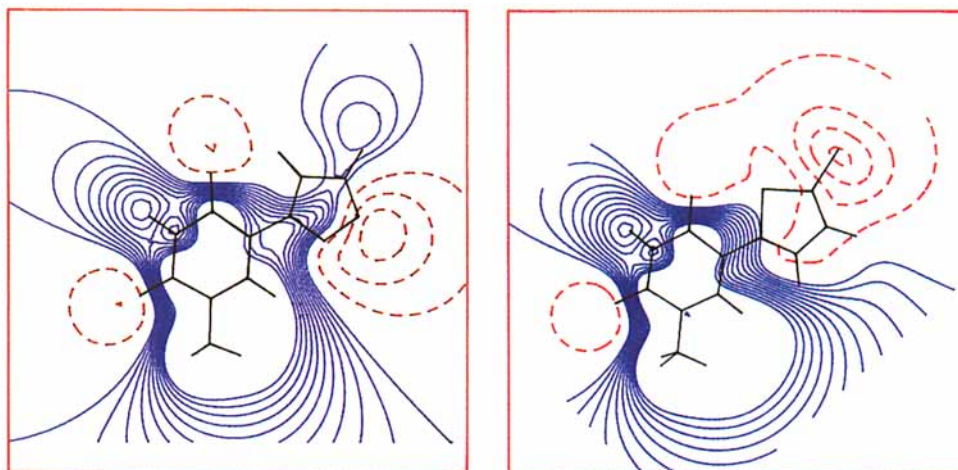


Fig. 3. Molecular electrostatic isopotential contour maps 1.75 Å above the plane of the rings of a) a compound with low affinity (2'-deoxy-5-(isoxazol-5-yl)uridine (**19**)) and of b) a compound with high affinity (2'-deoxy-5-(5-chlorothien-2-yl)uridine (**5**)) for thymidine kinase. Negative equipotential regions describe favourable interaction energy and are given in dashed lines; positive equipotential regions are given in solid lines. The contour-to-contour interval for the negative and positive isocontours are 5 and 1 kcal·mol⁻¹, respectively.

The electrostatic isopotential contour map of 2'-deoxy-5-(isothiazol-5-yl)uridine (**12**) 1.75 Å above the plane is depicted in *Fig. 4*. This analysis predicts that **12** might have an excellent affinity for the TK, at least in the conformation **12A** as it fulfils the requirements for binding. This compound has been synthesized, and the prediction was borne out: **12** in solution mainly exists in conformation **12A** and has indeed a high affinity for the enzyme. However, **12** does not show any antiviral activity (*Table 1*). This compound is the only one from the whole series where no relationship is found between viral TK affinity and antiviral activity.

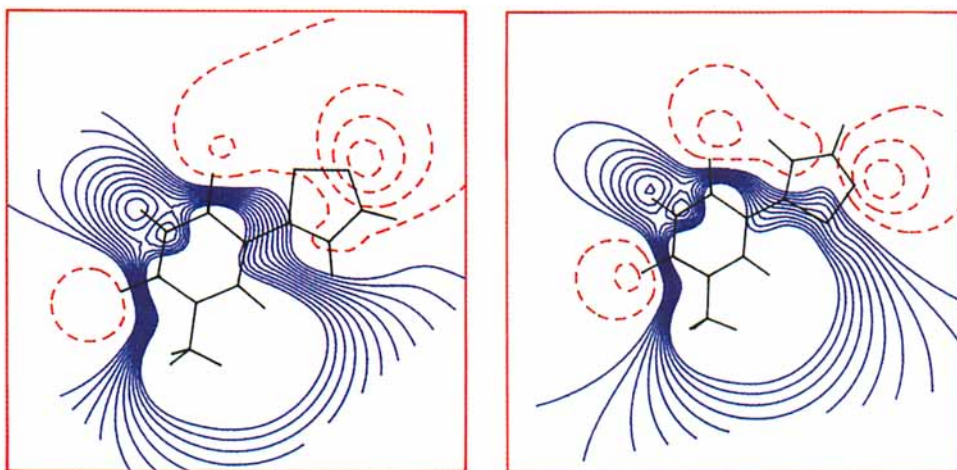


Fig. 4. Molecular electrostatic maps at 1.75 Å for 2'-deoxy-5-(isothiazol-5-yl)uridine in a) conformation **12A** and b) conformation **12B**. The contour-to-contour interval for the negative and positive isocontours are 5 and 1 kcal·mol⁻¹, respectively.

Results and Discussion. – 1. *Synthesis and Structural Analysis.* Before the crystal structure of TK was available, 2'-deoxy-5-(isothiazol-5-yl)uridine (**12**) with conformation **12A** (Table 2) was predicted to have strong affinity for HSV-1 TK. This prediction was based on the calculated potential, the dipole moment (Table 2), and the molecular electrostatic maps (Fig. 4) of conformers **12A** and **12B**. The difference in energy between conformer **12A** and **12B** is *ca.* 4 kcal/mol. Conformer **12A** fulfils the previously derived electronic characteristics that are important for the interaction with HSV-1 TK: a) the

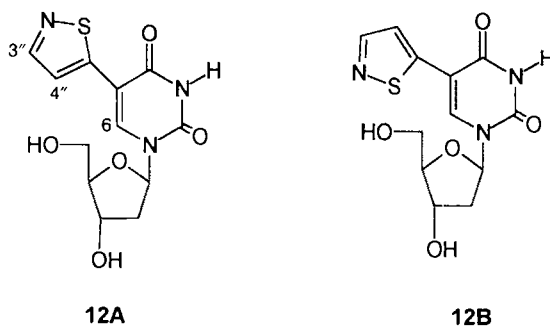


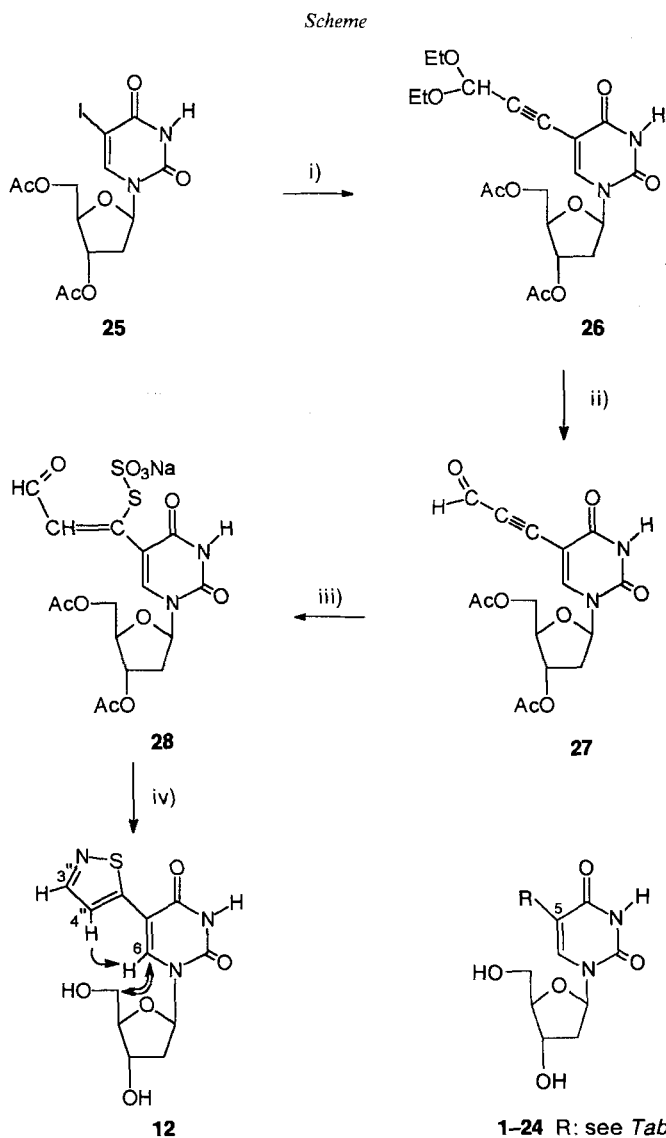
Table 2. Calculated Energy and Dipole Moment of Conformers **12A** and **12B**

	12A	12B
Energy [au] ^{a)}	-1005.4429	-1005.4364
Dipole moment [D]	4.3	3.0
Orientation ^{b)}	identical	not identical

^{a)} The energy difference between the two conformers is *ca.* 4 kcal/mol at the 3-21G level. ^{b)} Orientation of the dipole moment compared to that of (*E*)-BVDU.

presence of a large attractive region 1.75 \AA above the five-membered heterocycle and a repulsive region 1.75 \AA above the uracil ring and *b*) a suitable dipole-moment orientation.

Compound **12** was synthesized from 2'-deoxy-5-iodouridine (*Scheme*). The coupling of 3',5'-di-*O*-acetyl-2'-deoxy-5-iodouridine (**25**) with propiolaldehyde diethyl acetal was carried out in the presence of $[\text{PdCl}_2(\text{Ph}_3\text{P})_2]$, CuI , and Et_3N at 50° (\rightarrow **26**; 91% yield) [10], and the acetal group of **26** was deprotected with 80% aqueous acetic acid, giving



- i) $\text{CH}\equiv\text{CCH}(\text{OEt})_2$, $[\text{PdCl}_2(\text{Ph}_3\text{P})_2]$, CuI , degassed Et_3N , 50° ; 91% yield. ii) 80% aq. AcOH ; 51% yield.
 iii) $\text{Na}_2\text{S}_2\text{O}_3$. iv) liquid ammonia (13% yield).

compound **27** (51% yield). Finally, ring closure of the crude thiosulfate intermediate **28** [11] and deprotection of the OH groups in liquid ammonia gave the desired compound **12** (13% yield). Compound **12** was characterized by the usual combination of mass spectrometry and ^{13}C - and ^1H -NMR spectroscopy, including 2D NOESY experiments at 500 MHz. Assignment of most of the 1D ^1H -NMR signals was rather straightforward by means of their chemical shifts and multiplicities and also by a 2D DQFCOSY spectrum. These studies established that the conformation equilibrium of **12** in solution is shifted almost completely to conformation **12A**.

The important differentiation between $H-C(3'')$ and $H-C(4'')$ of **12** was firmly established by a H,C-hetero-correlation experiment as the ^{13}C -NMR chemical shifts for $C(3'')$ and $C(4'')$ are characteristic and well separated, and thus easily assigned. The conformation of the isothiazole ring with respect to the base was established by a 1D NOE difference experiment: saturation of $H-C(4'')$ at 7.62 ppm gives key enhancements at $H-C(3'')$ (7.9%) and $H-C(6)$ (7.8%) which clearly indicates the presence of conformation **12A**, in which $H-C(4'')$ and $H-C(6)$ are close to each other and the S-atom points towards the $C(4)=\text{O}$ group where it possibly can be stabilized by p,d-bonding interactions. The existence of strong NOE cross-peaks in the NOESY spectrum between $H-C(6)$ and $H_a-C(2')$ and also between $H-C(3'')$, $H_a-C(5')$, $H_b-C(5')$, and $OH-C(5')$ indicates that the orientation around the glycosyl bond shows a pronounced preference for 'anti'-conformation, as is usually observed for pyrimidine nucleosides. At the same time, this allows assignment of the most deshielded H-atom of $\text{CH}_2(2')$, i.e. $H_a-C(2')$ at 2.30 ppm to the H-atom *cis* to the nucleobase. NOE Cross-peaks between $H_a-C(2')$ and $H-C(3'')$, and between $H_b-C(2')$ (2.24 ppm) and $H-C(4'')$ and $OH-C(3'')$ confirm this assignment for $H_b-C(2')$ (or the $2'$ -H in the PSEUROT program notation) being the H-atom *trans* to the nucleobase.

The geometry of the furanose ring (Table 3) was determined from coupling constants $^3J(\text{H,H})$ (at 500 MHz) using the concept of pseudorotation [12–14] in which the conformation of a puckered five-membered ring is fully described by two parameters: a phase angle of pseudorotation P and a puckering amplitude Ψ_m . In solution, the furanose ring exists as an equilibrium of two rapidly interconverting conformers, called North-type ($P \approx 0^\circ$) and South-type ($P \approx 180^\circ$). Thus, four conformational parameters have to be determined, P_N , P_S , Ψ_{mN} , Ψ_{mS} , as well as the mol-fraction of each conformer. These parameters could be readily obtained from the $^3J(\text{H,H})$'s using the computer program PSEUROT (V. 6.2)¹⁾. Running PSEUROT based on the experimental J couplings (see Table 3) and using the standard Donders-generalized Karplus equation and other necessary *exo-endo* conversion parameters implemented in the program or in the accompanying database, revealed that compound **12** has a slight preference for a S-type puckered conformation in DMSO solution. This result is very similar to that for other deoxy-ribonucleosides in H_2O , although the population of the major or South-conformer usually is somewhat higher. It should be noted that in obtaining these results, which are collected in Table 3, the two puckering parameters for the N-type were held constant at the typical values for deoxynucleosides, i.e., $P_N = 14^\circ$ and $\Psi_{mN} = 38^\circ$ (between $C(3')$ -*endo*/ $C(2')$ -*exo* twist and $C(3')$ -*endo*-envelope structures), and only the S-type parameters and its molar fraction were optimized. Given the fact that we only had a single set of five experimental input values, the program was not instructed to optimize the five normally requested conformational parameters, since under such circumstances, the outcome of PSEUROT is quite sensitive to experimental inaccuracies¹⁾.

2. Modelling Experiments. 2'-Deoxy-5-(isothiazol-5-yl)uridine (**12**) has strong affinity for HSV-1 TK (Table 1). To investigate the structural features which could explain this affinity, a structural study of the HSV-1 TK enzyme in complex with **12**, and a comparison with dThd was undertaken. Of the two most likely conformers of **12**, conformation **12A** was found to be *ca.* 4 kcal/mol more stable than conformation **12B** (Table 2).

¹⁾ The translation of coupling constants J to P and Ψ_m is achieved in three steps, all incorporated in the PSEUROT program; *i*) The generalized Karplus equation (Donders modification) relates the $^3J(\text{H,H})$ values with the corresponding H,H-torsion angles $\Phi(\text{H,H})$ and takes into account the effect of substituent electronegativity and orientation; *ii*) the H,H exocyclic torsion angles $\Phi(\text{H,H})$ are related to the corresponding endocyclic torsion angles ν_i by the equation: $\Phi(\text{H,H}) = a_{\nu_i} + b$; *iii*) The endocyclic torsion angles ν_i are translated into the phase angle of pseudorotation P and the puckering amplitude Ψ_m according to equation: $\nu_i = \Psi_m \cos(P + (i - 2)144^\circ)$ with $i = 1-4$ [15].

Table 3. Calculated Pseudorotation Parameters (P, Ψ_m), Molar Fraction (x), and Theoretical Values of the Coupling Constants $J(H,H)$ and H,H -Torsion Angles $\Phi(H,H)^a$ for the Two Conformers N/S and a Comparison of the Total Calculated Coupling Constants (J_{calc}) with the Experimental Values (J_{exp}) at 500 MHz

	Conformer N		Conformer S		J_{exp}	J_{calc}	$\Delta J = J_{\text{exp}} - J_{\text{calc}}$
	$J(H,H)$	$\Phi(H,H)$	$J(H,H)$	$\Phi(H,H)$			
$J(1',2')$	1.37	98.4	10.06	152.5	6.00	6.21	-0.21
$J(1,2'')$	8.04	-21.9	5.74	31.7	6.40	6.76	-0.36
$J(2',3')$	6.68	40.7	5.07	-32.6	6.00	5.78	+0.22
$J(2'',3'')$	9.72	161.2	0.80	87.9	4.90	4.75	+0.15
$J(3',4')$	8.54	-163.4	0.66	-98.6	3.80	4.15	-0.35
P [°]	14.0		164.1			r.m.s. = 0.26 Hz	
Ψ_m [°]	38.0		32.7			r.m.s. = 0.26 Hz	
x	0.43		0.57			r.m.s. = 0.26 Hz	

^a) Using the PSEUROT procedure⁽¹⁾ V.6.2, and based on the experimental $^3J(H,H)$'s measured at 500 MHz. The overall root-mean-square error of the fit was 0.26 Hz.

Table 4. Decomposition of the Total Interaction Energy, under the Form of Non-Bonded van der Waals and Electrostatic Terms, between **12A** or dThd and HSV-1 TK into Contributions of Separate Residues

Residue	Relative contribution to the total interaction energy ^{a)}	
	12A	dThd
	Glu-83	-0.28
Tyr-101	-0.10	-0.08
Gln-125	-0.15	-0.13
Tyr-172	-0.13	-0.13
Arg-222	+0.13	+0.12
Glu-225	-0.21	-0.19

^a) Interaction energy between the particular residue and substrate divided by the total interaction energy between the whole enzyme and the substrate. A dielectric constant $\epsilon = 1$ was used. For more details, see *Exper. Part*.

Therefore, **12A** was docked into the active site of HSV-1 [16] and subsequently subjected to energy minimization to optimize its orientation. Of the total interaction energy between TK and the substrate (dThd or **12A**), 90% stems from the interaction with only six residues. These residues and their relative interaction energies are listed in Table 4. A structural comparison between the crystal structure of the TK-dThd complex [16] and the minimized complex of TK with **12A** is shown in Fig. 5. The strengths of these interactions are of comparable magnitude in both dThd and **12A**. This reflects that the two substrates bind TK in a very similar fashion and that replacement of the Me group in dThd by a larger isothiazole moiety in **12A** has no significant effect on the binding orientation of **12A** when compared to dThd. Focussing on the interactions involving the pyrimidine moieties of the substrates, we find that the bases are stacked parallel to the phenol ring of Tyr-172, and that this interaction accounts for *ca.* 10% of the total interaction energy. This stacking interaction also orients the pyrimidine base of both substrates in the plane of the amino group of Gln-125, allowing formation of H-bonds to H-C(3) and C(4)=O of the bases. Taken together, the substrate base moieties contribute to *ca.* 30% of the total interaction energy, while the remaining 70% can be largely attributed to the sugar part of the substrates. These sugar moieties are mainly involved in interactions with

Tyr-101, Glu-83, and Glu-225. Residues Glu-225 and Tyr-101 are together responsible for nearly 30% of the total interaction energy, due to the formation of two strong H-bonds with the 3'-OH groups. However, the most important interaction is formed between Glu-83 and the 5'-OH function, contributing as such to almost $\frac{1}{3}$ of the total interaction energy for each substrate. On the other hand, for both substrates, repulsive interactions between Arg-222 and the 5'-OH groups are observed. Upon minimization of the TK-12A complex, the side chains of Tyr-132, Arg-163, and to a lesser extent, Ala-167, undergo a slight conformational shift (*Fig. 6*). This small rearrangement creates a large cavity lined by the side chains of Tyr-132, Arg-163, Ala-167, Ala-168, and which can be occupied by the isothiazole moiety of **12A** (*Fig. 6*). Inspection of *Figs. 5* and *6* indicates that C(3) of the isothiazole moiety is located in close proximity of the phenolic O-atom of Tyr-132 and the aliphatic part of the Arg-163 side chain.

3. *Biochemistry.* Compound **12** was inhibitory to HSV-1 TK at an IC_{50} of 3.1 μM in the presence of 1 μM [*methyl*- ^3H]dThd as the competing natural substrate. (*E*)-5-(2-Bromovinyl)-2'-deoxyuridine (BVDU; **23**) and (*E*)-2'-deoxy-5-(2-iodovinyl)uridine (IVDU) showed 50% inhibitory concentrations of 0.3 and 0.6 μM , respectively. Thus, **12** is endowed with a pronounced affinity for herpetic TK that is slightly inferior to the prototype antiherpetic agents BVDU and IVDU. However, from these experiments, it is not possible to deduce whether the test compounds act as inhibitors of the enzyme or as alternative substrates. Therefore, we examined the ability of HSV-1 TK to use **12** as a substrate by incubating the enzyme and **12** in a reaction mixture containing [γ - ^{32}P]ATP as the phosphate donor. Included as controls were thymidine and BVDU, which are known to act as substrates for the enzyme. 2'-Deoxy-5-(isothiazol-5-yl)uridine **12** clearly behaved as an alternative substrate for HSV-1 TK. Whereas BVDU was phosphorylated by HSV-1 TK at 60% efficiency of the natural substrate dThd, **12** was phosphorylated at 50% efficiency at all time points examined (*i.e.*, 15, 30, and 45 min). Thus, **12**, like BVDU, acts as an alternative substrate for the HSV-1-TK-catalysed phosphorylation reaction. In accord with the slightly higher IC_{50} of **12** than that of BVDU for HSV-1 TK using dThd as

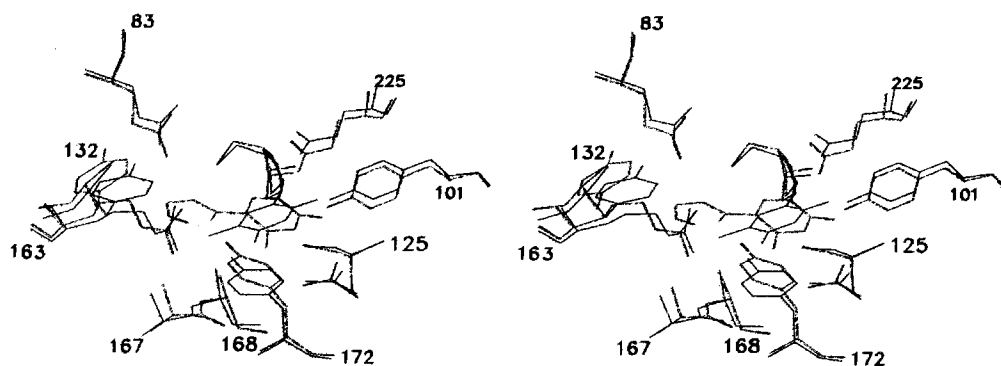


Fig. 5. Stereoplots of the minimized structure of HSV-1 TK in complex with **12A** (atom-colour coded) and superimposed onto the TK-dThd crystal structure of Brown et al. [16] (cyan-coloured). Only the residues which contribute significantly to the binding of substrates, or the residues which are shifted in the TK-12A complex compared to their orientation in the TK-dThd complex, are shown.

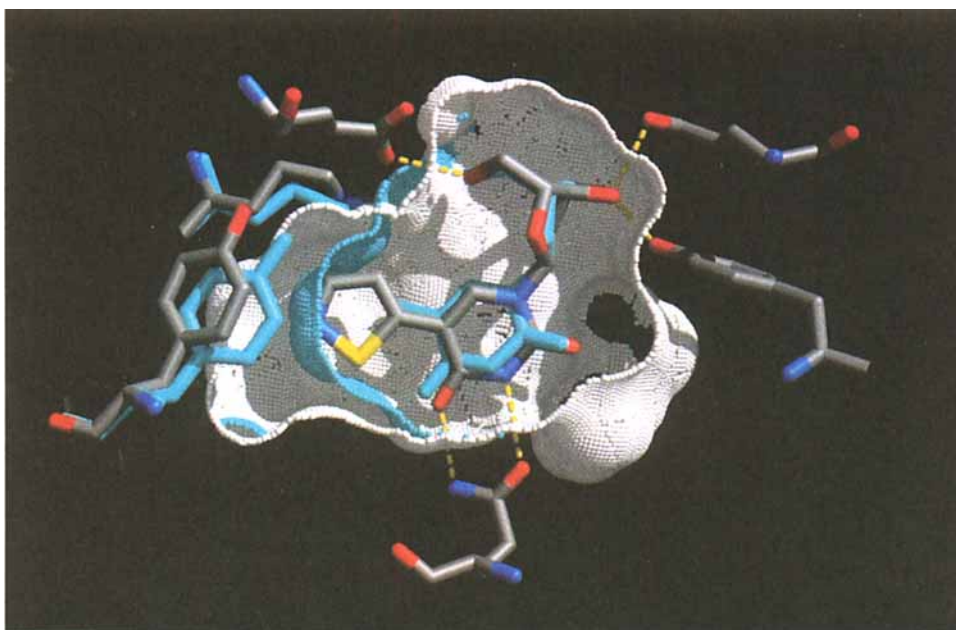


Fig. 6. Binding geometry of thymidine (cyan-coloured) in the active site of HSV-1 TK compared with the predicted binding orientation of 2'-deoxy-5-(isothiazol-5-yl)uridine (**12A**; atom-colour coded). H-Bonds are indicated by yellow dotted lines. The view shows a narrow slice through the active site of HSV-1 TK, and the surface of the pocket is drawn in white (**12A**) and cyan (dThd). Upon binding of **12A**, the side chains of Tyr-132 and Arg-163 (both on the left side of the picture) undergo a slight conformational shift (cyan-coloured are the conformations from the TK-dThd crystal structure and atom-colour coded are the predicted conformations for TK-**12A**). This small rearrangement creates a large cavity which can be occupied by the isothiazole moiety of **12A**.

the competing substrate, the phosphorylating capacity of HSV-1 TK for **12** was inferior to that of BVDU.

2'-Deoxy-5-(isothiazol-5-yl)uridine (**12**) was also evaluated for its cytostatic activity against murine mammary carcinoma FM3A tumor cells that were transfected with the HSV-1-TK gene and express the HSV-1 TK in the cytosol. In sharp contrast with BVDU, **12** lacked any marked inhibitory effect on both wild-type (FM3A/0) and HSV-1-TK-gene-transfected FM3A TK-/HSV-1 TK⁺ cells ($IC_{50} > 50 \mu\text{g/ml}$). Under similar experimental conditions, BVDU was *ca.* 10 000-fold more cytostatic against the FM3A TK-/HSV-1 TK⁺ than against the FM3A/0 cells. Earlier studies revealed that the latter phenomenon could be ascribed to a potent and selective inhibitory effect of BVDU 5'-monophosphate on thymidylate synthase in the intact cells [17] [18]. These findings were in agreement with the observed inhibitory effect of BVDU 5'-monophosphate against purified thymidylate synthase from murine leukemia LI210 cells and represent an example of an antiviral compound that is a marked inhibitor of thymidylate synthase [2]. Therefore, we may infer that the 5'-monophosphate derivative of **12** is not inhibitory to thymidylate synthase. Indeed, 5-substituted 2'-deoxyuridines may exhibit a structure-activity relationship for the viral TK that is different from that of their 5'-monophosphates for thymidylate synthase.

Conclusion. – Since the discovery of 2'-deoxy-5-iodouridine as an antiviral nucleoside by Prusoff [1], numerous 5-substituted 2'-deoxyuridines were synthesized and evaluated as anti-herpes agents. These studies were largely done on an empirical basis. It is only since the recent availability of a series of 5-heteroaryl-substituted 2'-deoxyuridines and since the availability of X-ray data of HSV-1 TK that the work proceeded on a more rational basis. The present study demonstrates that some 5-substituted nucleoside analogues may be good substrates for the HSV-1-encoded thymidine kinase without showing antiviral activity. The antiviral activity of this class of nucleoside analogues is due to either inhibition of thymidylate synthase (following their conversion to the 5'-monophosphate form) or inhibition of HSV-1 DNA polymerase (after their conversion to the 5'-triphosphate form). In the present study, it was demonstrated that 2'-deoxy-5-(isothiazol-5-yl)uridine (**12**) is a substrate for the HSV-1-encoded thymidine kinase. Yet, indirect data suggest that in its 5'-monophosphate form, **12** did not prove inhibitory to thymidylate synthase in intact cells. Whether it is a substrate for further phosphorylation (to its 5'-di- and 5'-triphosphate) and, as 5'-triphosphate, an inhibitor or substrate of the viral or inferred DNA polymerase remains subject of further studies. Using molecular modelling, we could also demonstrate in which way **12** is actually bound to the herpes viral TK. The results of this study also confirmed the previously published hypothesis on the binding of ligands in the active site of herpes TK [6].

Experimental Part

1. *Chemistry. General.* TLC: precoated Macherey-Nagel-Alugram-Sil-G-UV₂₅₄ plates; detection by UV light and H₂SO₄/anisaldehyde spray. Column chromatography (CC): Janssen Chimica silica gel (0.060–0.200 nm). M.p.'s: in capillary tubes with a Büchi-Tottoli apparatus; uncorrected. UV Spectra: Philips-PU-8700-UV/VIS spectrophotometer. ¹H- and ¹³C-NMR Spectra: Varian-Gemini-200-MHz spectrometer; SiMe₄ as internal standard (¹H) and the solvent signal of (D₆)DMSO (39.6 ppm) or CDCl₃ (77.0 ppm) (¹³C); coupling patterns from first-order analysis; δ in ppm, J in Hz. ¹H-NMR for **12**: Varian-Gemini-500-MHz spectrometer; ca. 3 mM in (D₆)DMSO at 303°K; differential 1D NOE experiment with 5 s of irradiation time using decoupling power of 10 dB; the 2D NOESY spectrum was recorded by Dr. Hoffman at Varian Application Laboratory, Darmstadt, in the phase-sensitive mode with a relaxation delay of 2.2 s, using 320 increments, each of 4 K complex data points, and a mixing time (τ_m) of 500 ms; the exper. ³J(H,H)'s of **12** were translated and interpreted in terms of a rapid two-state equilibrium between a puckered N-type and S-type furanose ring with the computer program PSEUROT (V. 6.2), which is based on the pseudorotational concept and the generalized Karplus equation¹.

3,5-Di-O-acetyl-2'-deoxy-5-(oxopropynyl)uridine (**27**). To a degassed soln. of 3',5'-di-O-acetyl-2'-deoxy-5-iodouridine (10 g, 18.3 mmol) in degassed Et₃N (50 ml) at 50° in the presence of [PdCl₂(Ph₃P)₂] (25 mg) and CuI (25 mg) was added CH≡CCH(OEt)₂ (7.3 g, 56.9 mmol). After stirring for 2 h at 50°, the solvent was evaporated, the residue dissolved in CHCl₃, the soln. washed with 5% aq. EDTA soln. (2×) and H₂O (1×), dried (Na₂SO₄), and evaporated, and the residual oil purified by CC (silica gel, AcOEt/hexane 2:1): crude **26** (7.31 g, 91%). The acetal protecting group was removed by treatment of crude **26** with 80% AcOH/H₂O at r.t. overnight. The aldehyde was purified by CC (AcOEt/hexane 2:1): 3.1 g (51%) of **27**. UV (MeOH): 228, 290. ¹H-NMR (CDCl₃): 2.14, 2.20 (2s, 2 Me); 2.31 (*d*, ²J(2'a,2'b) = 14.3, ³J(2'b,1') = 6.6, H_b-C(2')); 2.65 (*ddd*, ²J(2'a,2'b) = 14.3, ³J(1',2'a) = 6.0, ³J(2'a,3') = 2.8, H_a-C(2')); 4.40 (*m*, H-C(4'), 2 H-C(5')); 5.25 (*m*, H-C(3')); 6.28 (*dd*, ³J(1',2'b) = 6.6, ³J(1',2'a) = 6.0, H-C(1')); 8.23 (*s*, H-C(6)); 9.38 (*s*, CH=O); 9.55 (*br. s*, NH). ¹³C-NMR (CDCl₃): 20.9 (2 Me); 38.7 (C(2')); 63.4 (C(5')); 73.5 (C(3')); 83.1 (C(1')); 86.4 (C(4')); 86.5, 93.0, 97.0 (C≡C, C(5)); 147.0 (C(6)); 148.8 (C(2)); 160.4 (C(4)); 170.2, 170.3 (2 C=O); 176.0 (CH=O). LST-MS (thioglycerol doped with NaCl) 365 ([M + H]⁺).

2'-Deoxy-5-(isothiazol-5-yl)uridine (**12**). A soln. of sodium thiosulfate pentahydrate (2.93 g, 11.62 mmol) in H₂O (3 ml) was added very slowly to a stirred mixture of **27** (3.8 g, 10.46 mmol), AcOH (0.5 g, 8.5 mmol), H₂O (20 ml), and acetone (10 ml). During the addition, the temp. was kept at –5 to 0°. After the addition, the mixture was kept for an additional 30 min at 0° and then evaporated. The residue (*cis/trans*-thiosulfate **28** (1:1) [11] by NMR) was not isolated, but immediately treated with liq. NH₃ (50 ml) at –70°. The resulting mixture was stirred

for a few h at -70° . Then the NH_3 was allowed to evaporate. The dark-coloured residue was extracted with MeOH (3×100 ml), the combined MeOH extract evaporated, and the residue purified by CC (silica gel, $\text{CH}_2\text{Cl}_2 \rightarrow \text{CH}_2\text{Cl}_2/\text{MeOH}$ 9:1): **12** (13% yield) which was crystallized from acetone. M.p. $> 250^\circ$. UV (MeOH): 260, 311. $^1\text{H-NMR}$ (D_6DMSO): 2.24 (*dd*(AB), $^2J(2'a,2'b) = 13.42$, $^3J(2'b,1') = 6.33$, $^3J(2'b,3') = 4.85$, $\text{H}_b\text{-C}(2'')$); 2.30 (*t*(AB), $^2J(2'a,2'b) = 13.44$, $^3J(2'a,1') = ^3J(2'a,3') = 6.13$, $\text{H}_a\text{-C}(2'')$); 3.68 (*dd*(AB), $^2J(5'a,5'b) = 11.96$, $^3J(5'b,4') = 3.07$, $^3J(5'b,\text{OH}) = 4.65$, $\text{H}_b\text{-C}(5'')$); 3.77 (*dd*(AB), $^2J(5'a,5'b) = 11.96$, $^3J(5'a,4') = 3.17$, $^3J(5'a,\text{OH}) = 4.75$, $\text{H}_a\text{-C}(5'')$); 3.87 (*dt*, $^3J(4',3') = 3.78$, $\Sigma(^3J(4',5'a) + ^3J(4',5'b)) = 6.24$, $\text{H-C}(4'')$); 4.35 (*dq*, $^3J(3',3'b) \approx ^3J(3',4') \approx ^3J(3',\text{OH}) = 4.36$, $^3J(3',2'a) \approx 5.75$, $\text{H-C}(3'')$); 5.28 (*d*, $^3J(3',\text{OH}) = 4.44$, $\text{OH-C}(3'')$); 5.45 (*t*, $^3J(5'a,\text{OH}) \approx ^3J(5'b,\text{OH}) = 4.65$, $\text{OH-C}(5'')$); 6.19 (*t*, $^3J(1',2'a) = ^3J(1',2'b) = 6.13$, $\text{H-C}(1'')$); 7.62 (*d*, $^3J(4'',3'') = 1.98$, $\text{H-C}(4'')$); 8.45 (*d*, $^3J(3'',4'') = 1.88$, $\text{H-C}(3'')$); 9.00 (*s*, $\text{H-C}(6)$); 12.00 (*s*, NH). $^{13}\text{C-NMR}$ (D_6DMSO , 200 MHz): 40.7 (C(2'')); 60.6 (C(5'')); 69.4 (C(3'')); 85.5 (C(1'')); 87.8 (C(4'')); 106.2 (C(5'')); 116.9 (C(4'')); 138.0 (C(6)); 149.3 (C(2'')); 155.8 (C(3'')); 157.1 (C(5'')); 161.8 (C(4')). LSI-MS (matrix DMSO): 312 ($[M + \text{H}]^+$). Anal. calc. for $\text{C}_{12}\text{H}_{13}\text{N}_3\text{O}_5\text{S}$: C 46.30, H 4.21, N 13.50; found: C 46.59, H 4.28, N 13.24.

2. *Molecular Modelling. General.* The 2.8-Å resolution crystal structure of HSV-1 thymidine kinase in complex with thymidine (dThd) [16] was used as starting point for all subsequent molecular-modelling experiments because of the high structural similarity between dT and **12A**. Only the first structure (A) in the asymmetric unit was used. H-Atoms were added using MacroModel [19], and dThd was removed prior to any docking or minimization calculations. Polar H-atoms of Ser, Tyr and Thr residues were repositioned manually based on geometrical and H-bonding criteria. All His residues were assumed to be neutral, and geometrical and H-bonding criteria were used to decide between the two tautomeric configurations. Atomic partial charges for the substrate **12A** were obtained by first optimizing the geometry at the STO-3G level of theory, followed by a single-point calculation to obtain the atomic partial charges from the electrostatic potential [20]. Visualization was done using MidasPlus [21] and MacroModel [19], while energy calculations were performed with the BatchMin module of MacroModel using their AMBER 3 parameters. *Ab initio* calculations were performed using GAMESS [22]. All modelling experiments were run on a Silicon Graphics-R8000 computer.

Docking of 2'-Deoxy-5-(isothiazol-5-yl)uridine (12A). 2'-Deoxy-5-(isothiazol-5-yl)uridine **12A** was built using molecular graphics and positioned in the active site of HSV-1 TK so that the orientation of its 2'-deoxyuridine moiety closely resembled that of dThd. In this orientation, the isothiazole moiety of **12A** made close contacts with the aliphatic side chain of Arg-163 and the phenolic ring of Tyr-132. The nucleobase formed two H-bonds with Glu-125 through atom N(3) and C(4)=O. This orientation was then optimized by means of energy minimization until the energy gradient dropped below 0.025 kcal/mol Å. In this procedure, residues within 15, 14, and 12 Å of dT of **12A** were constrained to their crystal-structure positions using a parabolic force constant of 10, 50, and 25 kcal/mol Å², respectively, while all residues within 8 Å of **12A** were allowed to move freely to account for the flexibility of the binding pocket. All other residues were omitted from the calculations. Nonbonded cutoff distances were 7 and 12 Å for *van der Waals* and electrostatic interactions, resp. A dielectric constant of $\epsilon = 1$ was used.

3. *Cells.* FM3A Cells (designated FM3A/0) derived from a spontaneous murine mammary carcinoma in a C3H/He mouse and FM3A/TK⁻ cells selected for resistance against 5-bromo-2'-deoxyuridine and lacking host cell thymidine kinase (TK) activity were maintained in RPMI 1640 culture medium containing 10% fetal calf serum and 2 mM L-glutamine, as previously described [18]. The FM3A TK⁻/HSV-1 TK⁺ cell line, lacking cellular TK activity and containing the HSV-1 TK gene was derived from FM3A/TK⁻ cells as reported earlier [18]. The culture conditions of the cells were mentioned above.

4. *Radiochemicals.* [*methyl*-³H]Thymidine (specific radioactivity 70 Ci/mmol) was provided by Moravek Biochemicals Inc. (Brea, CA). [γ -³²P]ATP (specific radioactivity 800 Ci/mmol) was obtained from ICN (Asse-Relegem, Belgium).

5. *Inhibition of Cell Proliferation.* The methods for evaluating the cytostatic effects of the test compounds against FM3A/0 and FM3A TK⁻/HSV-1 TK⁺ cells have been reported previously and were based on the determination of the number of cells after a 48-h incubation period at 37° [23].

6. *Enzyme Source.* Herpes simplex virus type 1 TK was derived from murine mammary carcinoma FM3A tumor cells that were made deficient for cytosolic TK but were stably transfected with the HSV-1 TK gene. Purification of HSV-1 TK from these tumor cells has been described earlier [24]. The enzyme derived from CC (DEAE-sepharose, 17-fold purification) was used for the determination of the 50% inhibitory concentration of the test compounds against the phosphorylation of [*methyl*-³H]dThd. The enzyme derived from the 3'-dTMP-sepharose affinity chromatography (53000-fold purification) was used for examination of the phosphorylating capacity of the enzyme for the test compounds.

7. *Enzyme Assays.* Partially purified HSV-1 TK enzyme was used to determine the 50% inhibitory concentration of the test compounds. The reaction mixture (50 μ l) consisted of 30 μ l of 50 mM Tris · HCl (pH 8.0) containing 2.5 mM MgCl₂, 10 mM DTT, 1 mg/ml BSA, 2.5 mM ATP, and 10 mM NaF, 5 μ l of test compound (*i.e.* BVDU, IVDU, or **12**), 2.5 μ l of phosphate-buffered saline (PBS), and 5 μ l of [*methyl*-³H]dThd (1 μ M; 0.125 μ Ci). The reaction was initiated by addition of 7.5 μ l of HSV-1 TK to the mixture and allowed to proceed for 15 min at 37° after which a 25- μ l aliquot was spotted on *Whatman-DE81*-filter discs. The filters were subsequently washed three times for 5 min in EtOH, and radioactivity was determined by scintillation counting. Affinity-chromatography-purified HSV-1 TK was used to examine the phosphorylating capacity of the enzyme against the test compounds. The reaction mixture (50 μ l) consisted of 30 μ l of 50 mM Tris · HCl (pH 8.0) containing 2.5 mM MgCl₂, 10 mM DTT, 1 mg/ml BSA, and 10 mM NaF, 5 μ l of dThd, BVDU, or **12** at 1 μ M, 8 μ l of Milli-Q H₂O, 2 μ M [³²P]ATP (1 mCi/ml), and 5 μ l of enzyme. At 0, 15, 30, and 45 min after initiation of the reaction, 10 μ l was spotted on PEI plates, and the phosphorylated products were separated from radiolabeled ATP by TLC (BuOH/AcOH/H₂O 2.5:1:1, 4-h run). The plates were dried and the radiolabeled spots cut out and counted for radioactivity. The retention times of dTMP, BVDU-MP and the monophosphate of **12** were *ca.* 0.37–0.40. [³²P]ATP remained at the start of the chromatograms.

We are grateful to Dr. D. Brown and Dr. M. Sanderson for providing us with the X-ray data of herpes viral TK. We thank Anita Van Lierde, Frieda de Meyer, and Lizette van Berckelaer for excellent technical assistance and Mieke Vandekinderen for editorial help. These investigations were supported by the *Belgian Fonds voor Geneeskundig Wetenschappelijk Onderzoek (F.G.W.O.)*.

REFERENCES

- [1] W. H. Prusoff, *Biochim. Biophys. Acta* **1959**, *32*, 295.
- [2] J. Balzarini, E. De Clercq, M. P. Mertes, D. Shugar, P. F. Torrence, *Biochem. Pharmacol.* **1982**, *31*, 3673.
- [3] P. Wigerinck, L. Kerremans, P. Claes, R. Snoeck, P. Maudgal, E. De Clercq, P. Herdewijn, *J. Med. Chem.* **1993**, *36*, 538.
- [4] P. Wigerinck, C. Pannecouque, R. Snoeck, P. Claes, E. De Clercq, P. Herdewijn, *J. Med. Chem.* **1991**, *34*, 2383.
- [5] P. Wigerinck, R. Snoeck, P. Claes, E. De Clercq, P. Herdewijn, *J. Med. Chem.* **1991**, *34*, 1767.
- [6] A. Olivier, I. Creuven, C. Evrard, G. Evrard, M. Dory, A. Van Aerschot, P. Wigerinck, P. Herdewijn, F. Durant, *Antiviral Res.* **1994**, *24*, 289.
- [7] I. Luyten, L. Jie, A. Van Aerschot, C. Pannecouque, P. Wigerinck, J. Rozenski, C. Hendrix, C. Wang, L. Wiebe, J. Balzarini, E. De Clercq, P. Herdewijn, *Antiviral Chem. Chemother.* **1995**, *6*, 262.
- [8] I. Creuven, C. Evrard, A. Olivier, G. Evrard, A. Van Aerschot, P. Wigerinck, P. Herdewijn, F. Durant, *Antiviral Res.* **1996**, *30*, 63.
- [9] A. S. Jones, S. G. Rahim, R. T. Walker, E. De Clercq, *J. Med. Chem.* **1981**, *24*, 759.
- [10] M. Robins, P. Barr, *Tetrahedron Lett.* **1981**, *22*, 421.
- [11] R. Raap, *Can. J. Chem.* **1966**, *44*, 1324.
- [12] C. Altona, M. Sundaralingam, *J. Am. Chem. Soc.* **1972**, *94*, 8205.
- [13] C. Altona, M. Sundaralingam, *J. Am. Chem. Soc.* **1973**, *95*, 2333.
- [14] C. A. G. Haasnot, F. A. A. M. de Leeuw, C. Altona, *Tetrahedron* **1980**, *36*, 2783.
- [15] F. A. A. M. de Leeuw, C. Altona, *J. Comput. Chem.* **1983**, *4*, 428.
- [16] D. G. Brown, R. Visse, G. Sandhu, A. Davies, P. J. Rizkallah, C. Melitz, W. C. Summers, M. R. Sanderson, *Nature Struct. Bio.* **1995**, *2*, 876.
- [17] J. Balzarini, E. De Clercq, A. Verbruggen, D. Ayusawa, K. Shimizu, T. Seno, *Mol. Pharmacol.* **1987**, *32*, 410.
- [18] J. Balzarini, E. De Clercq, *Meth. Find. Exp. Clin. Pharmacol.* **1989**, *11*, 379.
- [19] F. Mohamadi, N. G. J. Richards, W. C. Guida, R. Liskamp, M. Lipton, C. Caufield, G. Chang, T. Hendrickson, W. C. Still, *J. Comput. Chem.* **1990**, *11*, 440.
- [20] U. C. Singh, P. A. Kollman, *J. Comput. Chem.* **1984**, *5*, 129.
- [21] T. E. Ferrin, C. C. Huang, L. E. Jarvis, R. Langridge, *J. Mol. Graphics* **1980**, *6*, 13.
- [22] M. W. Schmidt, K. K. Baldrige, J. A. Boatz, S. T. Elbert, M. S. Gordon, J. H. Jensen, S. Koseki, N. Matsunaga, K. A. Nguyen, S. J. Su, T. L. Windus, M. Dupuis, J. A. Montgomery, *J. Comput. Chem.* **1993**, *14*, 1347.
- [23] J. Balzarini, C. Bohman, R. T. Walker, E. De Clercq, *Mol. Pharmacol.* **1994**, *45*, 1253.
- [24] J. Bohman, J. Balzarini, P. Wigerinck, A. Van Aerschot, P. Herdewijn, E. De Clercq, *J. Biol. Chem.* **1994**, *269*, 8036.